Hyperfine Interactions 74(1992)193–204

A LASER ION SOURCE FOR ON-LINE MASS SEPARATION

P. VAN DUPPEN, P. DENDOOVEN, M. HUYSE and L. VERMEEREN
Instituut voor Kern- en Stralingsfysica, K.U. Leuven, Celestijnenlaan 200 D, B-3001 Leuven, Belgium

Z.N. QAMHIEH, R.E. SILVERANS and E. VANDEWEERT
Laboratorium voor Vaste Stof-fysika en Magnetisme, K.U. Leuven, Celestijnenlaan 200 D, B-3001 Leuven, Belgium

A laser ion source based on resonance photo ionization in a gas cell is proposed. The gas cell, filled with helium, consists of a target chamber in which the recoil products are stopped and neutralized, and an ionization chamber where the atoms of interest are selectively ionized by the laser light. The extraction of the ions from the ionization chamber through the exit hole and skimmer is similar to the ion-guide system. The conditions to obtain an optimal system are given. The results of a two-step one-laser resonance photo ionization of nickel, and the first results of laser ionization in a helium buffer gas cell are presented.

1. Introduction

Experiments at on-line mass separators are often limited by the release characteristics of the element of interest and by the isobaric contaminants present in the final beam. This can be illustrated by an example: the doubly-magic, neutron-rich ^{78}Ni could be produced in a particle-induced fission reaction in quantity, enabling the study of its decay characteristics. Although the primary production looks promising, the production of a secondary beam of ^{78}Ni is not straightforward. The half-life of ^{78}Ni is estimated to lie around 150 ms and this will cause severe decay losses during the diffusion out of the target and the ionization in the ion source. Furthermore, the $A = 78$ mass chain will be overwhelmed by more stable isobars. This problem is not specific to the fission process; also beams of extreme neutron-deficient isotopes produced by heavy-ion-induced reactions suffer from the same drawback.

In the case of nickel, the production of beams of short-living isotopes is limited by the delay in the target-catcher-ion-source system, whereas in other cases, such as the refractory elements, the release characteristics are even totally preventing the production of a secondary beam.

The existence of these problems was already realized in the early days of on-line mass separators [1]. A more universal and a faster thermalization and ionization scheme is the ion-guide technique [2]. The reaction products, recoiling out of the thin target, are thermalized in helium; during the thermalization process, the charge of the stripped ions is reset to a 1^+ state. If the ion survival time is of the same order

as the ion transport time out of the reaction and thermalization chamber into the isotope separator, a high efficiency for the production of a secondary beam can be achieved. For instance, in light-ion-induced fusion reactions, for which the recoil energy is low, a total efficiency between 1% and 10% can be reached for all elements and for nuclei with half-lives as short as 1 ms [2]. However, the major drawback of the ion-guide technique is that, due to the short ion survival time, only the nuclei, stopped in the region near the exit hole, are evacuated as 1^+ ions, excluding stacks of targets and long thermalization chambers for energetic recoils.

Several possibilities to obtain chemical selectivity have been developed. For example, by cooling the transfer line between the target and the ion source one succeeded in producing very pure beams of noble gases, as has been shown at ISOLDE [3]. Another way to improve the selectivity of a catcher-ion source system is by making use of the fact that some elements are easily and some are badly released from the catcher material. This method was used successfully at the GSI isotope separator [4]. However, these and other solutions are applicable only in very specific cases and sometimes give only a moderate reduction of the contaminants.

Resonance photo ionization with lasers (further referred to as laser ionization) provides in principle isotopically and isobarically pure ions because it uses resonant excitation of the atoms. Depending on the available lasers, it is possible to obtain an ionization efficiency near unity for about 80% of all elements, i.e. every atom that is irradiated by the laser(s) will be ionized [5]. In order to obtain this high efficiency, relatively high laser powers are needed, depending of course on the way the laser ionization is performed. So far, only pulsed lasers can deliver this high power. These lasers have one major drawback, namely their low duty-cycle (10^{-4}–10^{-7}). Since the production of radioactive nuclei at isotope separators such as LISOL [6] is continuous, the maximum overall efficiency will only be 10^{-4}. Several methods have been proposed to solve this problem. The activity can be deposited on a surface and then be desorbed with an ablation laser that works synchronously with the ionizing laser [7–9], or the activity can be stored in a moderately heated cavity, preventing the atoms from condensation at the walls of the chamber. The low temperature limits the amount of surface ionization and a laser beam is sent into the chamber through a small exit hole [10, 11].

In this contribution, we propose a method that combines the fast and universal thermalization of reaction products in a gas and the high selectivity of laser-based ionization by using the ion storage capacity of noble gases to overcome the low-duty cycle problem. Noble gases have the nice property to store atoms *as well as* 1^+ ions for a certain time. In other words, if one can store the atoms in between laser pulses in, for example, helium and extract the ions out of the helium (like it is done in the ion-guide technique [2]), one has in principle an optimal system.

We will present the results of a feasibility study for a laser ion source at LISOL, based on ionization in a gas cell. The principle of the proposed laser ion source is given in section 2. The ionization cross section of nickel using a one-laser system will be discussed in section 3. The first test results of laser ionization in a

gas cell filled with helium are presented in section 4. In section 5, off-line studies with the ion guide are described. Both section 4 and section 5 contain information on the flow patterns in the gas cell, necessary for the final design of the laser ion source.

2. Principle of the proposed laser ion source

We will first describe the laser ion source in general terms before giving some specific numbers on the dimensions of the chamber and the expected evacuation times. The problems related to diffusion losses will be addressed in a separate section.

2.1. GENERALITIES OF THE LASER ION SOURCE

A schematic drawing of how such a laser ion source might look is shown in fig. 1. The recoil products from a fusion–evaporation reaction or fission reaction (only the former is shown in the figure for reasons of simplicity) are stopped in the

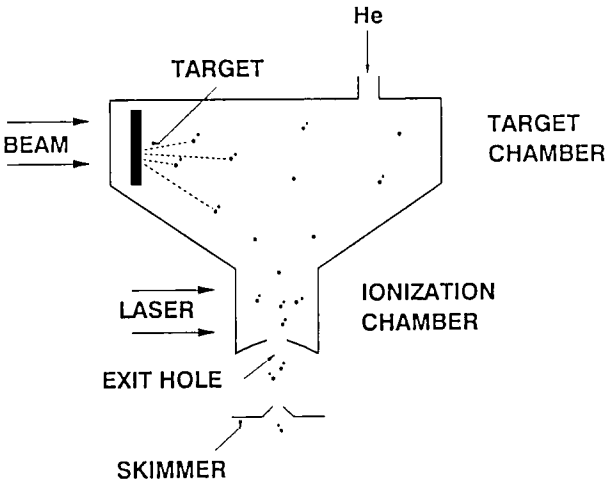

Fig. 1. Schematic layout of the proposed laser ion source. The exit hole and skimmer are identical to the ion-guide system [12].

helium gas of the target chamber and are transported together with the helium gas to the ionization chamber. The recoil products thermalize as neutrals or as 1^+ charged ions, but after a few milliseconds (typically 2 ms), all the ions are neutralized [12]. If we make the transport time from the target chamber to the ionization chamber longer than the ion survival time, all the reaction products will be neutralized before they arrive in the ionization chamber. The short ion survival time is believed to be due to recombination with the plasma electrons created by the projectile beam in the target chamber [13]. Especially in the case of heavy-ion-induced reactions, this

effect is dramatic: the energy loss of e.g. a ^{16}O(210 MeV) beam in helium is more than one order of magnitude higher than the one of a 15 MeV proton beam. In the ionization chamber, the atoms of interest are selectively ionized by the laser light; the other atoms are essentially unaffected. The ions are then transported by the helium flow through the exit hole, behind which most of the helium is removed by the skimmer (differential pumping) and the ions are accelerated towards the analyzing magnet of the separator, a situation identical to the ion-guide system. Note that the primary beam does not pass the ionization chamber: this region is essentially free of plasma electrons and the ion-survival time will become longer than ~10 ms [13]. A process that has been neglected so far is the loss of ions and atoms due to diffusion to the walls of the target and/or ionization chamber. This problem will be addressed later.

By choosing the volume of the ionization chamber and the exit-hole diameter in such a way that the evacuation time (τ_e) of the ionization chamber equals the time between two laser pulses (t_{rep}) and that τ_e is smaller than the ion-survival time (τ_{ion}), one obtains an optimal system:

$$\tau_{ion} \geq \tau_e \geq t_{rep}. \tag{1}$$

In this case, every atom is irradiated at least once by the laser and every ion that is created will survive its transport to the exit hole. In order to stop energetic recoil products like in heavy-ion fusion evaporation reactions, pressures in the target chamber ($P_{t.ch.}$ in hPa) higher than 500 hPa have to be used. This is a factor of five higher than in conventional ion-guide systems. Because of the gas load limit of the LISOL separator, currently Q_{max} = 100 hPa l/s, the exit-hole diameter is limited. The conductance of the exit hole can be written as a function of the exit-hole diameter (ϕ_{exit} in mm): $C_{exit} = 0.45(\phi_{exit})^2$ in l/s and is independent of the pressure. This equation is valid only if the ratio between the pressure out and inside the gas cell is smaller than about 10%. This reveals $\phi_e \leq 0.7$ mm. The proposed target chamber is 3 cm long and has a cross-sectional area of 1 cm^2. The volume of the ionization chamber ($V_{i.ch.}$) is determined by the laser repetition rate:

$$V_{i.ch.} = t_{rep} \frac{Q_{max}}{P_{t.ch}} \times 1000 \quad [\text{cm}^3]. \tag{2}$$

For excimer lasers, t_{rep}^{-1} is typically 200 Hz and consequently $V_{i.ch.}$ = 1 cm^3, and for copper vapor lasers, t_{rep}^{-1} is around 10 kHz and $V_{i.ch.}$ = 0.02 cm^3. This means that the laser beam has to irradiate half a sphere around the exit hole with a radius of 0.78 cm (excimer laser) or 0.21 cm (copper vapor laser) depending on the type of laser used. Here, we assume that the helium flow inside the target and ionization chamber is homogenous. In order to make sure that the transport time between the target and the ionization chamber is longer than ~5 ms – all ions must be neutralized – we have to add an additional volume between these two chambers.

The total evacuation time of the laser ion source will then be about 23 ms in the case of an excimer laser and about 19 ms in the case of a copper vapor laser. Consequently, only nuclei with a half-life shorter than ~30 ms will suffer to a certain extent from decay losses in the laser ion source.

Another process that causes a reduction of the overall efficiency of the laser ion source is the formation of molecules by the recoil products with impurity atoms. Furthermore, when a recoil atom thermalizes in a metastable state while the the laser frequency is tuned to ionize starting from the atomic ground state, it will be unaffected by the laser light. A small admixture of H_2 or N_2 gas can quench the metastable states. Both processes can only be studied on-line; so far, this has not been performed.

2.2. DIFFUSION LOSSES IN THE LASER ION SOURCE

In order to get an idea of the losses due to diffusion to the walls of the chamber, one can consider the following. Since in the target chamber, part of the helium atoms are ionized by the impact of the primary beam, one can use the ambipolar interdiffusion of recoil ions through a different but ionized medium. An average value for this diffusion coefficient (D_a in cm^2/s) for all ions in helium at room temperature is given by [14]:

$$D_a = \frac{650}{P_{t.ch.}}. \tag{3}$$

With this diffusion coefficient one can solve the diffusion equation inside a sphere or a cylinder to get an idea of the spreading out of the ions in the target chamber. After a time τ (s), 1/e of the ions have diffused over a distance X (cm); X and τ are related as follows:

$$\tau = \frac{1}{D_a}\left(\frac{X}{2.4}\right)^2. \tag{4}$$

At a pressure of 500 hPa, the ions have diffused over a mean distance of ~3 mm in about 20 ms. If the evacuation of the chamber is homogeneous, then the losses due to diffusion to the walls of the chamber are small. However, using lower pressures might cause losses. This was evidenced by efficiency measurements for the ion-guide system using recoil products from α-decaying nuclei (see section 5 and ref. [6]). The efficiency measured as a function of pressure rises when going to higher pressures and seems to saturate at 175 hPa. This effect is interpreted as being due to diffusion losses since the diffusion coefficient is inversely proportional to the pressure (see eq. (3)).

On the other hand, if there exists a preferential flow regime inside the target and ionization chamber, then part of the gas cell will be evacuated much faster and the diffusion process has to be reexamined in view of these flow patterns (see section 4).

3. Selective two-step photo ionization of Ni

Because of the strong nuclear physics interest in the study of neutron-deficient nickel isotopes – approaching the double magic nucleus ^{78}Ni – we started to study the photo ionization of nickel. Other elements like manganese, cobalt, molybdenum and barium have also been investigated. For the laser ionization, we used the two-step one-color photo ionization technique, which was first used by Ambartsumyan et al. [15]. A full discussion of this technique may be found in ref. [5]. Two identical photons are subsequently absorbed by the nickel atom: resonant absorption of the first photon excites the nickel atom to a level above half of the ionization limit, before decaying to a lower energy level, the excited atom is ionized by absorbing a second photon of the same frequency.

The UV laser light was produced by a pulsed dye laser system. The second harmonic (532 nm) output of a Q-switched Nd:YAG (Quanta-Ray DCR-11) pulsed laser was used to pump a (Quanta-Ray PDL-3) dye laser with a DCM solution in methanol (620–660 nm output). Second harmonic generation (310–330 nm) of this output was obtained by frequency doubling using a wavelength extender (Quanta-Ray WEX-1). The power of the laser beam was measured using a calibrated thermopile. This thermopile was also used in combination with a movable knife edge, intersecting the laser beam, to measure its cross-sectional area. The 320 nm laser beam of 10 Hz repetition rate, about 10 ns pulse duraction time, and 3.5 mJ maximum energy per pulse was directed towards a vacuum chamber (10^{-6}–10^{-5} hPa) in which the nickel atoms were produced by resistive heating of a nickel wire of 1 mm diameter. No lenses were placed in between the wavelength extender and the vacuum chamber, the laser beam was approximately parallel over the interaction zone, and its cross-sectional area could be varied (1–4 mm^2) by changing the internal alignment of the dye laser. The ions were collected on a negatively-biased plate connected to a preamplifier system (Ortec 120).

We investigated the nickel resonance ionization using the two-step one-color scheme in the wavelength range 320–325 nm. Detailed results on the observed transitions are presented in [16]. In fig. 2, we show the number of nickel ions detected as a function of the laser energy for the 322.698 nm resonance transition. This is the strongest ground state originating transition, ionizing the nickel atoms via the $^3G_4$ excited state. The curve shows a fit through the data with the following function: $\alpha(1 - \exp(-\beta \times \text{energy}))$ (α and β are the fitting parameters). From this fit, an ionization cross section of $6.3(30) \cdot 10^{-17}$ cm^2 was obtained.

4. Photo ionization in a gas cell

In order to investigate the performances of the ionization chamber of the proposed laser ion source (fig. 1), we studied photo ionization in a gas cell similar to the ionization chamber. A schematic drawing of this cell is shown in fig. 3. The atoms of interest are created by heating a nickel filament. The filament is situated

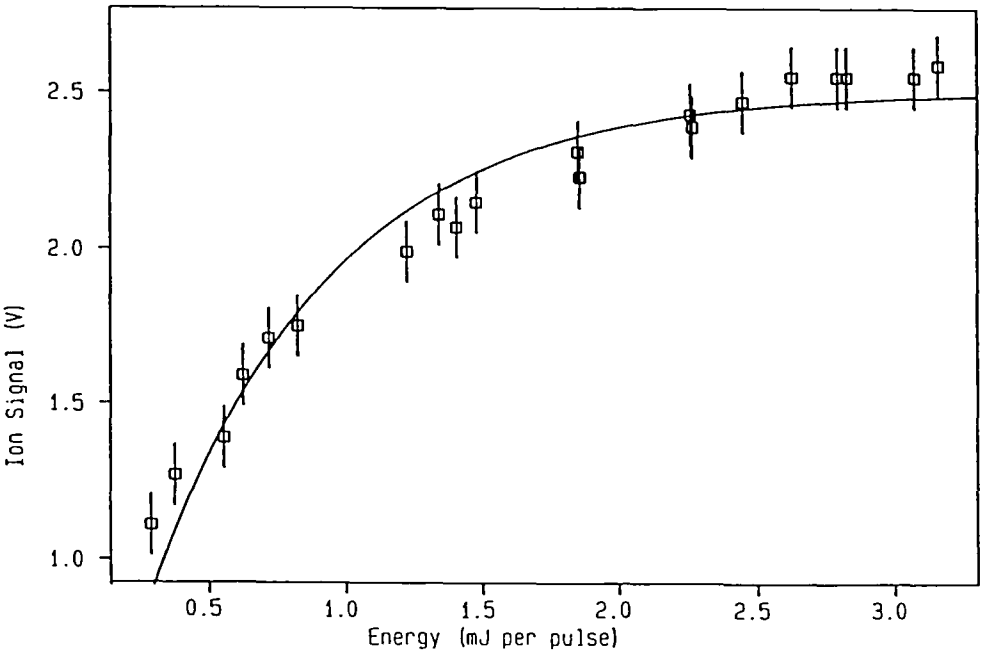

Fig. 2. Number of nickel ions (relative units) versus laser energy per pulse (322.698 nm line) using two-step one-color ionization. At high laser energies, the ionization step is almost completely saturated: approximately all nickel atoms that are irradiated by the laser are ionized.

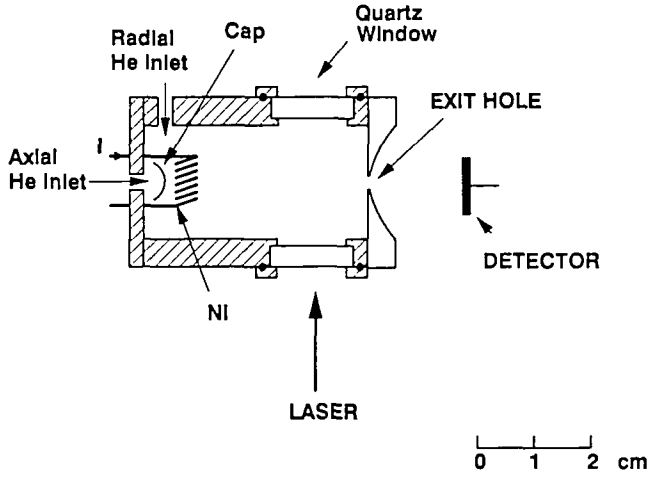

Fig. 3. Schematic drawing of the gas cell used for testing the resonant ionization in a buffer gas.

near the helium gas input. The gas input can either be radial or axial. The gas chamber was placed in a vacuum vessel that was pumped with a roots blower pump (Balzers WKP250). The temperature of the nickel wire was kept above 1100 K, depending strongly on the He flow rate. The sublimation rate for 1100 K is $6 \cdot 10^9$ atoms/second. The created atoms are carried by the helium flow towards the exit hole. In the region in front of the exit hole, the atoms are ionized by the laser beam entering (and leaving) the gas cell through two quartz windows. Once the ions have crossed the exit hole, they are collected on a negatively biased plate (~−50 V) and detected. The ion signals were monitored on a digital memory oscilloscope. Typical ion signals with the laser tuned on-resonance, for different distances between the position of impact of the laser beam and the exit hole, are shown in fig. 4. When

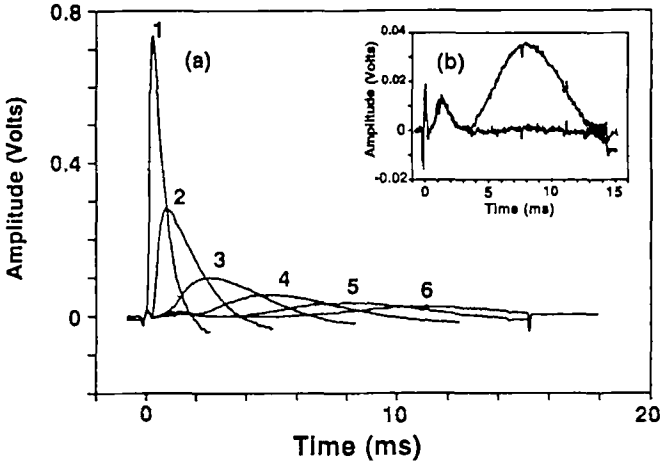

Fig. 4. The amplitude of the on-resonance ion signal (322.698 nm) at different distances between the laser beam and the exit hole as a function of the time elapsed since the impact of the laser beam (a). Curves 1 through 6 correspond to distances d = 2, 4, 6, 8, 10 and 12 mm. The inset (b) shows the on-resonance and off-resonance signal at d = 10 mm (curve 5). Pressure inside the gas cell is 600 hPa, and the exit hole diameter is 0.5 mm.

the laser was tuned off-resonance (see inset fig. 4), background pulses of less than typically 2% relative to the on-resonance signal were observed. The non-resonant component around 2 ms is rather independent of the distance to the exit hole and was also present without heating of the nickel filament. This non-resonant signal is most probably due to ionization of rest gases in the vacuum chamber surrounding the gas cell (typical pressure 10^{-1}–10^{-2} hPa). The integral of the ion pulse is proportional to the number of ions detected, e.g. the pulse at 10 mm corresponds to about $3 \cdot 10^7$ ions. The response of the preamplifier system was measured using a fast pulse generator: decay time constant 52 μs, rise time smaller than 100 ns.

Deconvolution of the pulses with this response will allow one to obtain the time behavior of the real ion pulse. From this, the evacuation time of the gas cell can be derived and different aspects that have an influence on the evacuation time (diffusion, shape of the exit hole and the gas cell) can be studied. This analysis is still in progress. As a first approximation for the evacuation time, we used the time for which the amplitude of the ion signal reaches a maximum. The flight time between the exit hole and the detector is considered to be negligible. The polarity of the heating current for the filament had no influence on the evacuation time. By performing another measurement during which the exit hole was completely shielded from the electrical field created by the voltage on the detector, we concluded that this electrical field had only a minor influence on the time behavior. Figure 5 shows

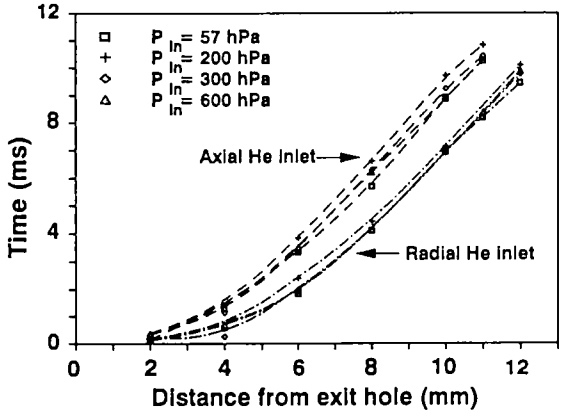

Fig. 5. The time elapsed between the moment of impact of the laser beam and the moment the ions are detected as a function of the distance between the position of the laser beam and the exit hole (ϕ_{exit} = 0.5 mm). Data are shown for different pressures and for radial as well as axial gas inlet. The laser beam was moved parallel to the central axis of the gas cell. The lines are drawn to guide the eye.

the extracted evacuation time (t in ms) as a function of the distance (d in mm) between the position of the laser beam and the exit hole (ϕ_{exit} = 0.5 mm). The laser beam is moved parallel to the central axis of the gas cell. One notices that the evacuation time is rather insensitive to the pressure inside the gas cell (as expected from the pressure independence of the conductance) and that there is a difference between radial and axial gas inlets. If we assume that the gas cell is evacuated in a homogeneous way, we can calculate from simple principles the time it takes for an ion formed at a distance d from the exit hole to be evacuated from the cell. The evacuated volume is a function of d and of the cross-sectional area of the gas cell. Consequently, the expression for t becomes: $t = 0.70\ d/(\phi_{exit})^2$. One notices that the

ions are evacuated much faster, as expected; at $d = 10$ mm, the time is expected to be 28 ms, while from the experiment one obtains a value between 7 and 10 ms (see fig. 5). When moving the laser beam perpendicular to the central axis, one notices an increase in the evacuation time for ions that are created away from the central axis of the gas cell (fig. 6). Data are shown for axial gas input; in the case of radial

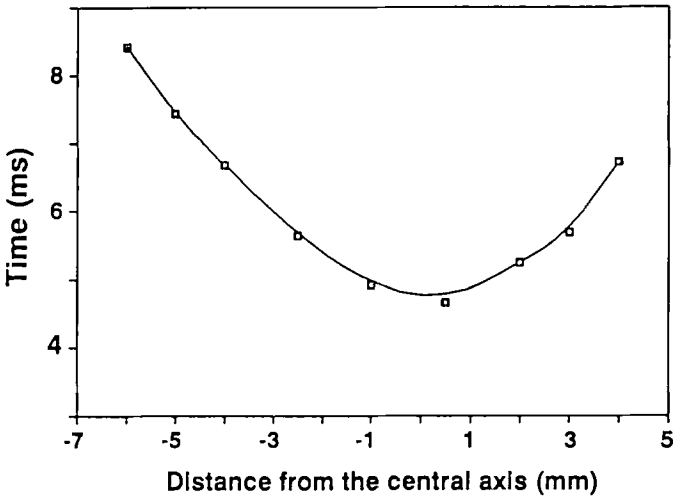

Fig. 6. The time elapsed between the moment of impact of the laser beam and the moment the ions are detected as a function of the distance from the central axis. The laser was moved perpendicular to the central axis. Data were taken at $d = 10$ mm. The line is drawn to guide the eye.

input, the same trend was observed except for the fact that the curve was asymmetric with respect to the central axis. These data clearly support the existence of preferential flow patterns inside the gas cell that make the evacuation of certain regions faster compared to others. The number of detected ions per pulse showed a decreasing trend when either moving away from the exit hole (horizontal laser scan) or when moving away from the main axis (vertical laser scan). We could not disentangle the contributions due to an inhomogeneous nickel density distribution in the gas cell and due to ion recombination, the former contribution probably being the most important one. It should be noted that the data shown in this contribution were taken with an improved pumping system (having a higher capacity) compared to the data presented in ref. [16]. In addition, small leaks in the gas cell were detected and repaired. Probably, these are the two reasons why the measured evacuation times in [16] showed a pressure dependence. Nevertheless, the final conclusion from ref. [16], i.e. the evacuation of the gas cell is three to four times faster than expected, remains valid.

5. Ion survival in the ion guide

Ion survival times in the ion guide have been determined by measuring the response of a stable mass-separated ion beam to the time structure of the ion-generating primary beam [12, 13]. Two milliseconds after the primary beam, passing through the thermalization chamber, has been stopped, the intensity of the mass-separated ion beam drops to zero [12]. The ion survival time increases to more than 10 ms when the ion-creating beam is not passing through the thermalization chamber [13]. To avoid all the primary-beam related effects, we studied the evacuation of ionized recoil products from the α decay of ^{223}Ra inside the ion-guide system [6, 17]. A 1120 Bq 11.43 days ^{223}Ra source was obtained by recoil implantation from a ^{231}Pa target onto an Fe catcher foil. In one second, ~560 ^{219}Rn and ~200 ^{215}Po nuclei are recoiling out of a ^{223}Ra-Fe foil. This was determined by capturing the recoiling nuclei on a thin carbon foil and measuring the α activity of the carbon foil. The ^{223}Ra-Fe foil is then placed inside the ion guide. The daughter products penetrate in the ion-guide chamber, thermalize in the helium gas to a 1^+ charge state and are mass separated. The ratio between the number of mass-separated ions versus the number of recoiling atoms then determines the efficiency of the ion guide. Efficiency tests have been done as a function of the catcher foil to exit hole distance (2, 5 and 11 mm opposite to the helium inlet, and 5 and 17 mm at the side of the helium inlet), the helium pressure (25–200 hPa), the exit hole conductance (0.65, 1.0 and 1.3 cm^3 per millisecond), and the skimmer voltage (0–600 V). Although the recoil products are thermalized within 5 mm of 100 hPa helium, the maximum of 40% efficiency for ^{219}Rn is only reached at 175 hPa. As already explained in section 2.2, we think this is evidence for diffusion losses. Time information on the ion-guide method can be obtained by comparing the efficiencies for ^{219}Rn ($T_{1/2}$ = 3.96 s) and ^{215}Po (1.78 ms). When the ^{223}Ra source is 5 mm from the exit hole, the Rn efficiency is 3.5 times higher than the Po efficiency. This can be understood by decay losses during the evacuation of the recoil volume (roughly 2 ms for a 1 cm^3/ms exit hole conductance). This simple explanation does not hold any longer when the catcher foil is at 17 mm distance from the exit hole. While the losses, due to the longer hold-up time in the thermalization chamber, for ^{219}Rn are limited to diffusion and recombination losses, an extra loss factor for the short-lived ^{215}Po should be present, thus the relative Rn to Po efficiency ratio should increase at least by one order of magnitude. Surprisingly, this ratio is identical. This could be understood by the existence of preferential, fast evacuating flow patterns inside the ion-guide thermalization chamber, as also was observed in the laser gas cell.

6. Conclusion

In this paper, we described a possible layout of a laser ion source based on resonance photo ionization in a gas cell. Hereby, the problems related to the low-duty cycle of pulsed laser systems – that have to be used for efficient laser

ionization – are dealt with by storing the atoms of interest in between laser pulses in a cell filled with noble gas (helium). The only condition that has to be fulfilled is an equality between the inverse of the laser repetition rate, the evacuation time of the ionization chamber and the ion survival time. We have studied the ionization of nickel atoms using the two-step one-color photo ionization technique. Ionization efficiencies near unity were obtained. The measurements in the laser gas cell and the ion-guide system seem to indicate that inside such a cell, flow channels exist. This flow pattern might force us to modify the design of our laser ion source and to use lasers with a high repetition rate, e.g. copper vapor lasers. On the other hand, a preferential flow pattern can also give some interesting new possibilities. By overlapping the preferential flow channel with the laser beam, the total ionization efficiency can be increased. Furthermore, the delay time of the ion source will be considerably smaller and diffusion losses will be reduced. An investigation in this direction is is progress.

References

[1] H.L. Ravn and B.W. Allardyce, On-line mass separators, in: *Treatise on Heavy-ion Science*, Vol. 8, ed. D.A. Bromley.
[2] J. Ärje, J. Äystö, H. Hyvönen, P. Taskinen, V. Koponen, J. Honkanen, A. Hautojärvi and K. Vierinen, Phys. Rev. Lett. 54(1985)99.
[3] H.L. Ravn, Phys. Rep. 54(1979)201.
[4] R. Kirchner, O. Klepper, D. Marx, G.E. Rathke and B. Sherrill, Nucl. Instr. Meth. A247(1986)265.
[5] G.S. Hurst and M.G. Payne, *Principles and Applications of Resonance Ionization Spectroscopy* (I.O.P. Publ. Ltd, 1988).
[6] M. Huyse, P. Decrock, P. Dendooven, J. Gentens, G. Vancraeynest, P. Vandenberghe and P. Van Duppen, *Proc. EMIS XII Conf.*, Sendai, 2–6 Sept. 1991, Nucl. Instr. Meth., to be published.
[7] U. Krönert, St. Becker, Th. Hilberath, H.-J. Kluge and C. Schulz, Appl. Phys. A44(1987)339.
[8] J.K.P. Lee, J.E. Crawford, V. Raut, G. Savard, G. Thekkadath, T.H. Duong and J. Pinard, Nucl. Instr. Meth. B26(1987)444.
[9] W.M. Fairbank and H.K. Carter, Nucl. Instr. Meth. B26(1987)357.
[10] F. Ames, T. Brumm, K. Jager, B.M. Suri, H. Rimke, N. Trautmann and R. Kirchner, Appl. Phys. B51(1990)200.
[11] G.D. Alkhazov, L.Kh. Batist, A.A. Bykov, V.D. Vitman, V.S. Letokhov, V.I. Mishin, V.N. Panteleyev, S.K. Sekatsky and V.N. Fedosyev, Nucl. Instr. Meth. A306(1991)400.
[12] K. Deneffe, B. Brijs, E. Coenen, J. Gentens, M. Huyse, P. Van Duppen and D. Wouters, Nucl. Instr. Meth. B26(1987)399.
[13] P. Taskinen, H. Pentillä, J. Äystö, P. Dendooven, P. Hauho, A. Jokinen and M. Yoshii, Nucl. Inst. Meth. A281(1989)539.
[14] M.A. Biondi and S.C. Brown, Phys. Rev. 75(1949)1700.
[15] R.V. Ambartsumyan, A.M. Apatin, V.S. Letokhov, A.A. Makarov, V.I. Mishin, A.A. Puretskii and N.P. Furzikov, Sov. Phys. JETP 43(1976)866.
[16] Z.N. Qamhieh, R.E. Silverans, E. Vandeweert, P. Van Duppen, M. Huyse and L. Vermeeren, *Proc. EMIS XII Conf.*, Sendai, 2–6 Sept. 1991, Nucl. Instr. Meth., to be published.
[17] P. Dendooven, Doctoraatsthesis, K.U. Leuven (1992), unpublished.